Available online at www.sciencedirect.com

ScienceDirect

Transportation Research Procedia 14 (2016) 3631 – 3640

Transportation Research Procedia

www.elsevier.com/locate/procedia

6th Transport Research Arena April 18-21, 2016

VeloCité – Development of an energy storage system for an e-bike

Henning Wittig [a,*], Ralf Bartholomäus [a], Thomas Lehmann [a]

[a]*Fraunhofer Institut for Transportation and Infrastructure Systems, Dresden, 01069, Germany*

Abstract

Within the framework of the development of an energy storage system for a lightweight electric bicycle the electric behavior of LiFePO4 cells was investigated. We propose a systematic and efficient procedure for identification and parameterization of a cell model based on measurements in the time domain. An equivalent circuit model approach was adopted using parameters dependent on temperature and state of charge. The model was parameterized for a wide range of operational conditions concerning temperature, state of charge and cell current. Finally, the accuracy of the proposed model is shown by the comparison of simulation results with real measurements of the given cell using a highly dynamic driving cycle.

Peer-review under responsibility of Road and Bridge Research Institute (IBDiM)

Keywords: Micro electric mobility; e-bike; state estimation; battery modeling; LiFePO4 cathode

1. Introduction

In terms of sustainability, the bicycle is undisputed by far the most attractive transport. Apart from the minimum area consumption of the bike paths bicycle traffic is free from environmental impact.

As part of the funding initiative „Schlüsseltechnologien für die Elektromobilität (STROM)“ of the German Federal Ministry of Education and Research (BMBF) a new lightweight electrical bicycle was developed, which, compared to common e-bikes and pedelecs, stands out due to the synergy of several technical innovations in the

* Corresponding author. Tel.: +49-351-464-0671; fax: +49-351-464-0803.
E-mail address: henning.wittig@ivi.fraunhofer.de

Peer-review under responsibility of Road and Bridge Research Institute (IBDiM)
doi:10.1016/j.trpro.2016.05.431

areas of frame and wheelset, drive train, power control and battery. Finally, as a result of functional integration it sets new tones with respect to shape and design.

The following sections provide initially an overview of the development priorities of the presented project. Thereafter, the characteristic electrical behavior of LiFePO4-based Li-ion cells as well as an adequate model approach will be outlined. The process of cell characterization and parameter estimation is demonstrated as well as the use of the identified cell model in algorithms of battery management.

2. E-bike concept of the future: battery and drive train integrated invisibly

The Velocité project unites three main objectives:

- a novel electric drive using a brushless DC electric (BLDC) motor in the form of a circular segment located near the wheel rim,
- dimensionally optimized lightweight structures for frame and wheels with directly integrated drive components,
- as well as a durable, secure and robust battery storage system with integrated battery and energy management.

The comprehensive development approach allows what is missing in conventional e-bikes and pedelecs: a new, modern design and a system weight comparable to conventional bicycles. Within the framework of the three-year cooperation the project partners have succeeded in integrating the components of the drive train, which are the electric motor, power electronics, energy storage and battery and energy management system, almost invisible into a lightweight and stiff carbon frame and the wheels (Wittig et al. (2015)).

2.1. Electric motor

Centerpiece of the VeloCité is the EVO2 electric motor developed by the DriveXpert GmbH. The bobbin coils of the BLDC motor are located in the bicycle frame, while the bicycle wheel rim represents the rotor. On each side of the wheel rim 180 permanent magnets have been integrated. Thus, the back wheel is directly driven by the electric motor without the need of an additional transmission. The electric motor is designed for a power consumption of 500 W assuming a maximum air gap between rotor and stator of 2 mm and has a total weight of 2950 g.

During the development of the electric motor two different variants were examined:

- An implementation as a claw pole motor which is located along a circular segment of the wheel rim. The stator consists of consecutively arranged tooth elements (claws), which are enclosed by a common coil.
- An implementation as a BLDC motor in the form of a circular segment.

The latter has significant advantages. The uniform distribution of the individual electrical phases yields to an identical influence of the air gap tolerances on the phases. The electrical asymmetries caused by the air gap tolerances are much lower than in an arrangement with three concentrated electrical phases, whereby the rotor is less prone to “sticking” to one side of the stator. Thus, the air gap between stator and rotor could be reduced significantly to achieve the required torques.

Furthermore the stator can be processed as one-piece plate cross-sections, whereby all other mechanical tolerances of manufacturing and individual installation are eliminated. The guidance of the magnetic flux is significantly shortened. The radial height of the stator poles is similar to the one of the permanent magnets, meaning that all magnetic material within the area of influence of the stator is used at its best. Although the single-tooth covering is more complex it is state of the art regarding the manufacturability.

The motor controller developed by Trinamic Motion Control GmbH & Co. KG was designed for three-phase BLDC-/PMSM motors using a supply voltage up to 36 V and a continuous power of 500 W. The size of the controller has been optimized for the dimensions of 12 cm x 5,5 cm x 2,5 cm. This allows the controller to be directly integrated into the available space of the frame. The cooling of the power section is realized via direct mechanical contact to the frame. For an efficient operation the motor has been optimized for sinusoidal commutation. This is realized by the motor controller via field oriented current control that operates with a 20 kHz

frequency. Digital Hall sensors with low resolution are used for motor control, while the calculated angle of the rotor position is interpolated in order to achieve a higher resolution. The development of the current controller and the structure of the motor as a direct drive enable a four quadrant operation including recuperation.

2.2. Lightweight construction and design

The low overall weight of less than 13kg of the VeloCité is accomplished by the material-specific advantages of carbon as well as the system lightweight construction. An attractive design and customer benefits encourage the transfer from car to pedelec. Therefore the high energy requirements of the production of carbon can be compensated by the reduction of pollutants and CO2 emissions especially in urban traffic. According to Achternbosch et al. (2003) the production of carbon components has neither ecological advantages nor disadvantages in comparison to the production of aluminum components. Using the advantages of the material properties of carbon allows the development of an innovative transmission technology and therefore shows benefits from the perspective of sustainability compared to aluminum bicycle frames.

An important project goal was to develop an attractive design, suitable for everyday use. The special design of the motor enables to integrate the electric drive train into the load-bearing structure of the frame and the rear wheel. Consequently, no additional components like transmission or external wiring are necessary.

The production of the carbon lightweight rim of the rear wheel was carried out in a combined sandwich / blow molding process. A rim profile has been developed, which allows to integrate the rotor magnets into a high profile rim of a width of only 20 mm. Due to the special layer structure of the rim a very high rigidity of 120 N/mm could be achieved, which is necessary to resist the lateral motor forces. The special hub design ensures minimum bearing clearance. The whole rear wheel has a weight of about 1.800 g.

2.3. Energy storage and battery management system (BMS)

The expected breakthrough in all electromobility concepts, whether in passenger cars, commercial vehicle or e-bikes is closely linked to the solution of the energy storage problem. If current weak points like

- low energy and power density,
- high costs,
- restricted intrinsic safety and
- reduced service life

can be improved, electric vehicles will succeed in the market.

The battery storage system developed by the Fraunhofer IVI is based on K2Energy lithium iron phosphate cells (LiFePO4) in standard format 26650, offering fast charging capability and therefore are suitable for recuperation function. The selected cell chemistry addresses in particular the last two weak points and is characterized by

- Its thermal stability and intrinsic safety as well as
- a high cyclic stability and good ageing behavior.

These characteristics outweigh the minor disadvantages that arise due to the lower energy and power density, caused by the lower nominal cell voltage of $3.2\,V$, compared to the NMC materials. In order to achieve the required system voltage of $20\,\mathrm{V} \leq \mathrm{U} \leq 30\,\mathrm{V}$, eight cells were connected in series. Taking into account the required performance and the available installation space of the bicycle frame, the optimum battery capacity was achieved by an 8s3p interconnection of the cells. The parallel connection is carried out at the cell level, reducing the impact of production-related and ageing-related variations in the electrical characteristics between the cells already by the construction of the battery.

Table 1. Specification of the energy storage system (8s3p cell connection).

type	26650 High Capacity Cell
capacity (Ah)	7,8
nominal voltage (V)	25,6
discharge current (A)	30
max. discharge current 30s pulse (A)	78
charge current (A)	15
charge voltage cutoff (V)	29,2
discharge voltage cutoff (V)	20,0
operating temperature (°C)	$-20 \leq \vartheta \leq 60$

In order to ensure a largely modular design of the e-bike, the energy storage system has its own control unit (BMS). This contains all algorithms including the cell monitoring and the battery and energy management.

The BMS realizes the monitoring of battery current and voltage and temperature on cell level. Due to its digital signal transmission temperature measurement is less susceptible to interference and needs low application effort.

Due to the small installation space and thus restricted possibilities of specific heat dissipation, special emphasis was placed on a suitable monitoring concept. E.g. temperature peaks at the power resistors during balancing can reliably be detected and measures be taken. Furthermore the electronics are electrically isolated from the energy storage to prevent it from damage and guaranty safe operation of the entire system in case of short or open circuit.

Since a maximum amount of energy content has to be provided for driving support, energy efficiency is an important aspect of electronic design. In order to minimize the energy consumption of the BMS hardware and to avoid a stand-by-mode, the microcontroller is switched off automatically at rest.

3. Battery management algorithms

For monitoring and diagnosis of the energy storage system algorithms for on-line determination of non-measurable variables such as state of charge (SOC), state of health (SOH) and state of function (SOF) are implemented in the BMS. These are based on a model for simulating the electrical behavior of the cell. Because of their safety relevance as well as the demand for high system availability under all operating conditions, the determination of such models is a focus of each battery development.

3.1. Experimental

The experiments described in the following section were performed for identification, parameterization and validation of the model for simulating the electrical behavior of the LiFePO4 cell. In the 8s3p cell arrangement of the battery the temperature and voltage measurements can take place only at the level of parallel connections. Therefore, the advantage to reduce the impact of production-related variations in the electrical characteristics between the cells can also be used in the parameter estimation. Consequently, all tests were carried out on three parallel connected cells. To provide defined ambient conditions a climatic chamber was used. The tests were divided into two series of measurements.

At first the capacity Q_0 and the SOC characteristic was determined, which reflects the relationship between open-circuit voltage (OCV) U and the amount of charge Q stored in the cell. Therefore, the cell is charged/discharged gradually with a specific charge of $\Delta Q = 0.05 * Q_0$ and a charge/discharge current of $|I| = 15.6\ A$. Each charging or discharging step is followed by a rest period of $t_{rest} = 7200\ s$. The length of the rest period is chosen to minimize the overpotential due to diffusion in the electrolyte and charge-transfer reactions at the electrodes. Thus, upper and lower bounds of the open-circuit voltage can be determined. The charge and discharge pulses are interrupted when reaching the cutoff voltages $U_{max} = 4.0\ V$ and $U_{min} = 2.2\ V$ respectively. Because of the

overpotential caused by a charge/discharge current of $|I| = 15.6A$ it has to be reduced to $|I| = 7.8A$ to measure the upper and lower end of the SOC range. Using the upper and lower bounds of the open-circuit voltage two vectors $\overline{\boldsymbol{OCV}}$ and $\underline{\boldsymbol{OCV}}$ with a common reference vector $\boldsymbol{Q}$ can be calculated by linear interpolation. The open-circuit voltage results from the averaging of $\overline{\boldsymbol{OCV}}$ and $\underline{\boldsymbol{OCV}}$ (Fig. 1).

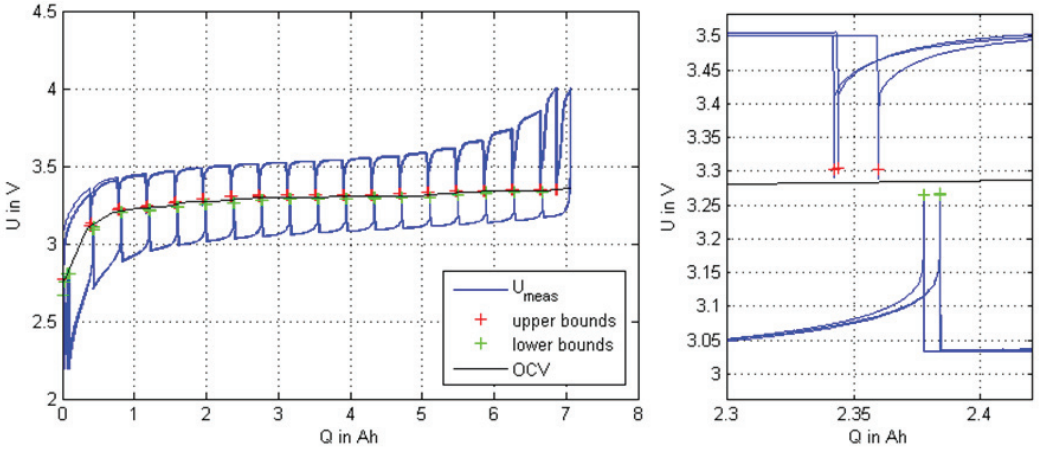

Fig. 1. Measurement data used for determination of SOC characteristic: measurement data (blue), upper bound (red), lower bound (green), SOC characteristic (black), left: entire measurement data of three charge/discharge cycles, right: detail to illustrate upper and lower bounds.

In order to analyze the behavior of the overpotential, the cells were tested using a load profile that cover the entire operational range of the SOC and the cell current I. The experiments were carried out at different ambient temperatures $\vartheta = 5°C, 20°C, 40°C$. The usage of a highly dynamic load profile guarantees high model accuracy under realistic application conditions. Nevertheless, the experiments were conducted at a constant ambient temperature, the cell temperature changes significantly due to power losses. This can be seen for example in Fig. 3, which shows the cell temperature during a driving cycle at $\vartheta = 20\ °C$. Therefore, the experiments described below contain several rest periods for relaxation of the cell temperature.

Test duration of each temperature was about 120 h, one third of which is used for parameter estimation and two thirds are used for validation. The experiment is divided into two sections, which are the load profile of 16 h and a rest period of 8 h. The load profile contains a random combination of the modi driving cycle, short rest period, charging ($I = 1.5\ A$) and fast charging ($I = 15.6\ A$).

Furthermore the load profile has the following characteristics:

- the cell is in a relaxed condition at the beginning of each test
- the current profile of the driving cycle uses the entire current range of the cell ($-10\ C < I < 2\ C$) according to the data sheet
- in case of violating the cut of voltages the current mode is aborted

The maximum charge and discharge currents are independent of the ambient temperature. Due to generally higher internal resistances at low temperatures and thus higher overpotentials, the SOC range is reduced at temperatures $\vartheta \leq 5\ °C$.

3.2. Dynamic model and parameter estimation

A detailed model of the electrical behavior of the cell is fundamental for almost all algorithms of the BMS including estimation of SOC, SOH and SOF. With regard to the application an abstract model approach has been adopted in the form of an equivalent circuit model, which offers a sufficiently high accuracy with acceptable model complexity. Thus, an appropriate model structure was developed, which is able to simulate all a priori known dominant effects (see Fig. 2). It consists of the main capacitor C_0 to store the charge Q, an ohmic resistance R_0 and the RC elements $R_1||C_1$, $R_2||C_2$, $R_3||C_3$ and $R_4||C_4$ to model the overpotentials $\eta := \eta_0 + \eta_1 + \eta_2 + \eta_3 + \eta_4$. The model parameters are dependent of the operating variables cell current I, cell temperature ϑ and cell $SOC = Q/Q_0$.

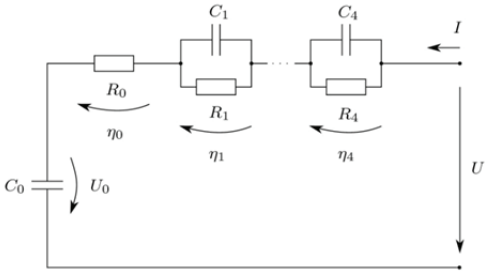

Fig. 2. equivalent circuit model of the lithium ion cell.

The open-circuit voltage OCV is a non-linear function of the SOC

$$OCV = h(SOC). \tag{1}$$

The RC elements have different time constants $\tau_k := R_k C_k$ $(k = 1, \dots, 4)$. Thus, the electrical behavior of the cell can be modeled both in highly dynamic stress periods with time constants in the range of a view seconds to minutes as well as in long-term load profiles or rest periods.

The model belonging to Fig. 2 results in a non-linear parameter estimation problem. With regard to the very long measurement series to be processed, the numerical treatment is highly demanding on system performance. Therefore a reduction to a linear parameter estimation problem was carried out. This includes the assumption that the time constants $\tau_k := R_k C_k$ $(k = 1, \dots, 4)$ of the RC elements are fixed and only the resistors are parameters of the estimation problem. When specifying the time constants the requirement $0 < \tau_1 < \tau_2 < \tau_3 < \tau_4$ is met, which means τ_1 is the smallest one (typically in the range of seconds) and τ_4 is the largest one (typically in the range of hours).

The ohmic resistance R_0 and the gains R_k of the RC elements are dependent on the current direction, which is indicated by the indices + (charge current) and – (discharge current). The associated time constants τ_k are the same for both current directions. The parameters R_3 and R_4 are only dependent on the temperature ϑ. This definition is motivated by the fact that the RC elements with large time constants τ_3 und τ_4 need an excitation time which inevitably causes a large SOC shift. Therefore, it is not possible to identify a SOC dependency of the parameters R_3 and R_4. As a result the model parameters are defined as

$$R_0^+ = R_0^+(\vartheta, SOC)$$
$$R_0^- = R_0^-(\vartheta, SOC)$$
$$R_{1/2}^+ = R_{1/2}^+(\vartheta, SOC)$$

$$\begin{aligned} R_{1/2}^{-} &= R_{1/2}^{-}(\vartheta, SOC) \\ R_{3/4}^{+} &= R_{3/4}^{+}(\vartheta) \\ R_{3/4}^{-} &= R_{3/4}^{-}(\vartheta) \end{aligned} \tag{2}$$

Consequently the state space formulation of the model equations can be expressed as:

$$\frac{d}{dt}\begin{pmatrix} SOC \\ \eta_1^+ \\ \eta_1^- \\ \vdots \\ \eta_4^+ \\ \eta_4^- \end{pmatrix} = \begin{pmatrix} 0 & 0 & 0 & \dots & 0 & 0 \\ 0 & -\tau_1^{-1} & 0 & \dots & 0 & 0 \\ 0 & 0 & -\tau_1^{-1} & \dots & 0 & 0 \\ \vdots & \vdots & \vdots & \ddots & \vdots & \vdots \\ 0 & 0 & 0 & \dots & -\tau_4^{-1} & 0 \\ 0 & 0 & 0 & \dots & 0 & -\tau_4^{-1} \end{pmatrix} \begin{pmatrix} SOC \\ \eta_1^+ \\ \eta_1^- \\ \vdots \\ \eta_4^+ \\ \eta_4^- \end{pmatrix} + \begin{pmatrix} \frac{1}{Q_0} & \frac{1}{Q_0} \\ \tau_1^{-1} & 0 \\ 0 & \tau_1^{-1} \\ \vdots & \vdots \\ \tau_4^{-1} & 0 \\ 0 & \tau_4^{-1} \end{pmatrix} \begin{pmatrix} \max\{I, 0\} \\ \min\{I, 0\} \end{pmatrix} \tag{3}$$

$$U = h(SOC) + \sum_{k=1}^{4} R_k^+ \eta_k^+ + \sum_{k=1}^{4} R_k^- \eta_k^- + R_0^+ \max\{I, 0\} + R_0^- \min\{I, 0\}. \tag{4}$$

The functions $\mathrm{R}_0^+, \mathrm{R}_0^-, \mathrm{R}_{1/2}^+, \mathrm{R}_{1/2}^-$ and $\mathrm{R}_{3/4}^+, \mathrm{R}_{3/4}^-$ are implemented using linear interpolation of 2D maps and 1D maps respectively.

The parameterization of the model is carried out in two steps. First, the SOC characteristic is determined as described in section 3.1. In the second step the remaining model parameters are fitted to measurement values using the least squares method. For a given current input signal $\mathrm{I}_{\mathrm{meas}}$, cell temperature $\vartheta_{\mathrm{meas}}$ and state of charge $\mathrm{Q}(0)$ at time $\mathrm{t} = 0$ the optimization problem can be expressed as

$$\min_{R_0^+, R_0^-, \dots, R_4^+, R_4^-} \sqrt{\sum_{i=1}^{n} |U(t_i) - U_{meas}(t_i)|^2} \tag{5}$$

Despite the large amount of data the parameter estimation is performed simultaneously for the entire operating range of the cell. Changes in the cell temperature, which cannot be avoided especially at low ambient temperatures, are taken into account by the estimation process. Furthermore, both measurement errors in the current signal as well as deviations between actual and estimated open-circuit voltage may have negative effects on the parameter estimation. Therefore, the steady state error between measured and simulated cell voltage is corrected in every rest period during the driving cycle using a filter algorithm. Finally, commonly known dependencies of the model parameters from the SOC and the cell temperature are used as constraints of the optimization problem to achieve the maximum accuracy already at low scope of measurement data. It is considered that the dependency of the parameters $\mathrm{R}_{\mathrm{k}}(\vartheta, SOC)$ on the SOC is described by a convex function. Furthermore, its dependency on the cell temperature ϑ decreases monotonically for increasing ϑ.

3.3. Model validation

The validation of the model is carried out at the load profiles described in section 3.1. For this purpose, the cell voltage U_{sim} is simulated based on the measured cell current I_{meas} and cell temperature ϑ_{meas}. U_{sim} is compared with the measured cell voltage U_{meas} in terms of the root mean square deviation RMS. This is calculated according to

$$RMS = \sqrt{\frac{1}{n}\sum_{i=1}^{n}(U_{sim}(t_i) - U_{meas}(t_i))^2}, \tag{6}$$

wherein $U_{meas}(t)$ and $U_{sim}(t)$ represent the measured and simulated cell voltage at time t respectively, and n is the number of measurement points.

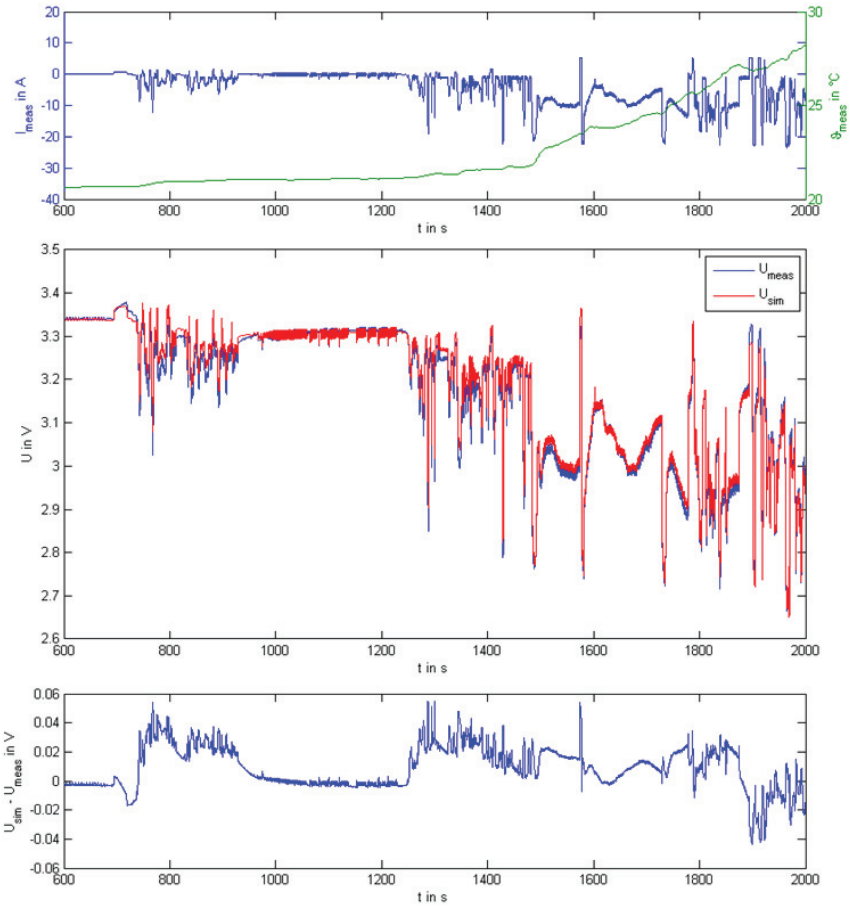

Fig. 3. comparison of measured and simulated validation data withdrawn from a driving cycle at 20 °C ambient temperature.

Fig. 3 shows measured and simulated signals on cell level during a driving cycle at an ambient temperature of $\vartheta = 20\,°C$. During the measurement the SOC is varying between $SOC_{start} = 95\,\%$ and $SOC_{end} = 25\,\%$. Temperature ϑ_{meas} measured at the surface of the cell increases due to power losses. The deviation between simulated and measured data $\varepsilon = U_{sim} - U_{meas}$ remains within $\varepsilon < 0.054\,V$. The RMS of the entire measurement is calculated to $RMS = 0.0198\,V$. In Fig. 4 the root mean square deviation as a function of the SOC interval is illustrated, which is less than $0.022\,V$ in a wide range of $20\,\% < SOC < 90\,\%$. In the peripheral areas of the SOC the cell shows a highly nonlinear behavior, which cannot be reproduced by the model structure and therefore increases the RMS significantly. Similar result were obtained for the ambient temperatures $\vartheta = 5\,°C$ and $\vartheta = 40\,°C$. Especially at $\vartheta = 5\,°C$ the SOC area of $SOC < 10\,\%$ was not covered during the measurements due to increasing overpotentials. However, model accuracy decreases in the lower areas of the SOC.

Over a wide range from $20\,\% < SOC < 90\,\%$ the accuracy of the model is sufficient. Further improvements are intended by taking into account the dependence of parameter $R_1 \ldots R_4$ on the cell current. This is subject of current research.

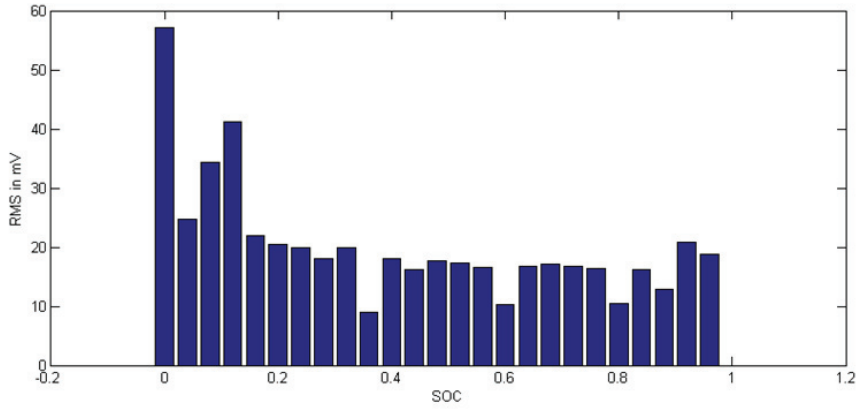

Fig. 4. RMS in dependence of SOC interval determined on the basis of validation data at an ambient temperature of 20°C.

3.4. Battery state estimation

In the field of traction applications battery management systems often estimate the SOC of the battery based on the open-circuit voltage or by coulomb-counting. These methods have large inaccuracies due to

- highly dynamic load profiles without sufficiently long rest periods to reach static conditions,
- unavoidable measurement errors, especially of the cell current, that accumulate during long load profiles.

The sensitivity of the SOC determination with respect to such problems is particularly large when the cell chemistry used (e.g. LiFePO4) has a very flat SOC-OCV-characteristic. Consequently, conventional systems often have to keep large reserves to the operating limits of the battery, which considerably limits the usable energy content. Solutions are offered by more sophisticated algorithms such as Extended Kalman filter (Plett (2004), Santhanagopalan et al. (2006)) or Unscented Kalman filter (Plett (2004)). However, discrepancies in the system properties (model uncertainty, process and measurement noise is not white and gaussian) can lead to significant estimation errors (Grewal et al. (2001)), which result in large, partly unfounded adjustments of the SOC.

To reduce estimation errors based on the described behavior a method was developed using observer-based algorithms, which allows for online determination of the internal cell state from the available measurement signals. Beside the information about the accuracy of the measured variables

- cell current I_{meas} (calculation of SOC via coulomb counting: $SOC = \int I_{meas} dt$) and
- cell voltage U_{meas} (calculation of SOC via SOC characteristic: $SOC = OCV^{-1}(U_{meas} - \sum_k \eta_k)$)

it uses especially a dynamic calculation of the model accuracy. Thus, a confidence interval of the simulated cell voltage can be determined providing information about the accuracy of the estimated SOC. The result is a more robust SOC estimation, which combines several advantages:

- correction of SOC estimation based on coulomb-counting also during load profile
- giving a reliable bound for estimated SOC
- increase in accuracy as measured data are weighted according to their information content

Nevertheless, computing and storage requirements are only slightly higher compared to approaches based on Kalman filter. In addition, the approach provides a basis for other algorithms of battery and energy management such as the estimation of SOH.

Within the scope of this paper the algorithm for SOC estimation can only be described qualitatively. A detailed analysis of the results will be published by the authors in a further paper.

4. Conclusion

The paper presents an overview of the development of a new lightweight electric bicycle. The combination of a novel electric drive which is integrated almost invisibly in the bicycles frame and rear wheel, optimized lightweight structures for frame and wheels with directly integrated drive components and a durable, secure and robust battery storage system results in an attractive design and a low overall weight of less than $13\ kg$.

Furthermore, a procedure for parameterization of an electric model for LiFePO4 cells was developed, suitable for application in an automotive BMS. The chosen model structure is a tradeoff between complexity and the ability to model the electric behavior of the cell within a wide range of operational conditions regarding SOC ($0\ \% < SOC < 100\ \%$), temperature ($5\ °C < \vartheta < 40\ °C$) and load current ($-10\ C < I < 2\ C$). This results in a linear parameter estimation problem which can be solved simultaneously for a large amount of measurement data from in total $120\ h$ with a sampling rate of $\Delta t = 0.1\ s$ collected in the entire operating range of the cell. The model accuracy was rated by the RMS of the deviation between measured and simulated cell voltage. It mainly depends on the SOC, whereas it is almost constant at $0.022\ V$ in a wide range of $20\ \% < SOC < 90\ \%$.

References

Achternbosch, M., Bräutigam, K.-R., Kupsch, C., Reßler, B., Sardemann, G., 2003. Analyse der Umweltauswirkungen bei der Herstellung, dem Einsatz und der Entsorgung von CFK- bzw. Aluminiumrumpfkomponenten. FZKA 6879, Wissenschaftliche Berichte, Forschungszentrum Karlsruhe GmbH, Karlsruhe.

CarboFibretec, 2014. „Die (R-)Evolution des E-Bikes“, www.carbofibretec.de/images/download/Pressemitteilung_Lightweight_Technologieprojekt_Velocite_ger.pdf.

Grewal, M. S., Andrews, A. P., 2001. Kalman Filtering – Theory and Practice Using MATLAB, in Wiley-Interscience Publication.

Plett, G. L, 2004. Extended kalman filtering for battery management systems of lipb-based hev battery packs, part 1, background, Journal of Power Sources, vol. 134 (2), pp. 252–261.

Plett, G. L, 2004. Sigma-point kalman filtering for battery management systems of lipb-based hev battery packs, part 1, Introduction and state estimation, Journal of Power Sources, vol. 161, pp. 1356–1368.

Santhanagopalan, S., White, R. E., 2006. Online estimation of the state of charge of lithium ion cell, Journal of Power Sources, vol. 161, pp. 1346–1355.

Wittig, H.; Thanner, S.; Dressler, E.; Bussinger, F., 2015. VeloCitè – Die (R-)Evolution des E-Bikes, conference proceedings: Urbane Mobilität der Zukunft, Symposium des Innovationsclusters REM 2030, Karlsruhe.